Dissecting the role of PtdIns(4,5)P_2 in endocytosis and recycling of the transferrin receptor

Namiko Abe[1,2], Takanari Inoue[2], Thierry Galvez[2], Lawrence Klein[3] and Tobias Meyer[2,*]

[1]Graduate Program in Neurosciences, Stanford University School of Medicine, Stanford, CA 94305, USA
[2]Department of Chemical and Systems Biology, Stanford University School of Medicine, Clark Center, 318 Campus Drive, Stanford, CA 94305, USA
[3]Graduate Program in Biophysics, and Department of Microbiology and Immunology, Beckman Center, 279 Campus Drive, Stanford University Medical School, Stanford, CA 94305, USA
*Author for correspondence (e-mail: tobias1@stanford.edu)

Accepted 21 February 2008
Journal of Cell Science 121, 1488-1494 Published by The Company of Biologists 2008
doi:10.1242/jcs.020792

Summary

Endocytosis and recycling of membrane proteins are key processes for nutrient uptake, receptor signaling and synaptic transmission. Different steps in these fission and fusion cycles have been proposed to be regulated by physiological changes in plasma membrane (PM) phosphatidylinositol (4,5)-bisphosphate [PtdIns(4,5)P_2] concentration. Here, we use a chemical enzyme-translocation strategy to rapidly reduce PM PtdIns(4,5)P_2 levels while monitoring clathrin-mediated endocytosis and recycling. PtdIns(4,5)P_2 hydrolysis blocked transferrin receptor endocytosis and led to a marked increase in the concentration of transferrin receptors in the PM, suggesting that endocytosis is more sensitive to changes in PtdIns(4,5)P_2 than recycling. Reduction of PM PtdIns(4,5)P_2 levels led to a near complete dissociation of Adaptor protein 2 (AP-2) from the PM but had only a small effect on clathrin assembly. This argues that receptor-mediated PtdIns(4,5)P_2 reduction preferentially suppresses AP-2-mediated targeting of cargo to endocytic sites rather than the assembly of clathrin coats or recycling of endocytic vesicles.

Supplementary material available online at
http://jcs.biologists.org/cgi/content/full/121/9/1488/DC1

Key words: Endocytosis, Phosphoinositides, Recycling

Introduction

Although phosphoinositides represent a minor fraction of cellular phospholipids, they are integral components of membranes and are believed to play key roles in cell signaling, cytoskeletal organization, vesicular transport and ion-channel regulation (Di Paolo and De Camilli, 2006; Suh and Hille, 2005). Among different phosphoinositide species, phosphatidylinositol (4,5)-bisphosphate [PtdIns(4,5)P_2] has been implicated in functioning as a second messenger that regulates clathrin-mediated endocytosis of receptors as well as recycling of internalized receptors back to the plasma membrane (PM) (Roth, 2004; Haucke, 2005; Di Paolo and De Camilli, 2006; Kim et al., 2006; Hinrichsen et al., 2003; Motley et al., 2003).

Although such a role of PtdIns(4,5)P_2 in endocytosis and recycling has been supported by a number of genetic and biochemical studies, PtdIns(4,5)P_2 has equally prominent roles as a cytoskeletal regulator and as a precursor for other second messengers, making it difficult to demonstrate that the observed effects of PtdIns(4,5)P_2 perturbations are direct. Long-term perturbations of PtdIns(4,5)P_2 levels might also cause changes in phosphatidylinositol (3,4,5)-trisphosphate [PtdIns(3,4,5)P_3], diacylglycerol and Ca^{2+} second messengers that alter gene expression and thereby indirectly interfere with endocytosis and recycling.

To overcome this limitation, we employed a rapamycin-induced hetero-oligomerization strategy to rapidly reduce the PM PtdIns(4,5)P_2 concentration within seconds. We and others have recently developed this method to test for a direct role of PtdIns(4,5)P_2 in ion-channel regulation (Suh et al., 2006), recruitment of proteins with polybasic residues (Heo et al., 2006), calcium signaling (Varnai et al., 2006) and endocytosis (Varnai et al., 2006; Zoncu et al., 2007). In this approach, PtdIns(4,5)P_2 is rapidly dephosphorylated by chemically inducible targeting of Inp54p, a PtdIns(4,5)P_2-specific 5′ phosphatase (Tsujishita et al., 2001), to the PM. The addition of iRap, a rapamycin analog (Inoue et al., 2005), causes dimerization of a PM-localized FKBP12-rapamycin binding domain (FRB) and a cytosolic Inp54p phosphatase domain conjugated to CFP and FKBP (CF-Inp) (Suh et al., 2006).

Here, we use this strategy to dissect the role of PtdIns(4,5)P_2 both in the internalization and recycling of transferrin receptors. We found that, although rapid reduction in PtdIns(4,5)P_2 concentration induced a near complete block of transferrin receptor endocytosis, bulk-phase endocytosis was not inhibited. Furthermore, the reduction in PtdIns(4,5)P_2 also enhanced the concentration of transferrin receptor at the PM, suggesting a preferential role of PtdIns(4,5)P_2 in regulating endocytosis over recycling. We further show that the clustering of transferrin receptors into coated pits is disrupted upon reduction of PtdIns(4,5)P_2 levels. PtdIns(4,5)P_2 reduction also dissociated the adaptor proteins AP-2, epsin and clathrin assembly lymphoid myeloid protein (CALM) from the PM, which is consistent with a role of PtdIns(4,5)P_2 in regulating AP-2 and possibly other adaptors in clustering transferrin receptors. Surprisingly, we found that this reduction in PtdIns(4,5)P_2 concentration has only a weak effect on the dynamic assembly of clathrin at the PM, suggesting that PtdIns(4,5)P_2 regulation is less important for the formation of clathrin coats. Together, our study suggests that reduction in PM PtdIns(4,5)P_2 concentration, as expected to occur upon receptor stimulation, first suppresses the adaptor-mediated targeting of cargo to endocytic sites before

interfering with dynamic assembly of clathrin coats and the recycling of internalized receptor.

Results

PtdIns(4,5)P_2 depletion blocks transferrin internalization

We first confirmed that rapid PtdIns(4,5)P_2 hydrolysis can be induced in HeLa cells, because we used this cell system for the study. Within seconds after iRap addition, CF-Inp translocated from the cytosol to the PM, whereas the PH-domain of PLCδ, which binds to PtdIns(4,5)P_2 with high specificity and affinity (Stauffer et al., 1998), dissociated from the PM, indicating a loss of PM PtdIns(4,5)P_2 (Fig. 1A,B). iRap-induced PtdIns(4,5)P_2 depletion in HeLa cells caused a near complete inhibition of the internalization of Alexa-Fluor-594-conjugated transferrin, consistent with a proposed role of PtdIns(4,5)P_2 in clathrin-mediated endocytosis (Fig. 1C,D). In control experiments, cells expressing CF-Inp and treated with DMSO instead of iRap still internalized transferrin (Fig. 1C,D). Furthermore, iRap-induced translocation of CF-Inp(D281A) (Suh et al., 2006), a phosphatase-dead mutant of CF-Inp, had little, if any, effect on transferrin uptake (Fig. 1C,D), suggesting that the inhibition of transferrin uptake by CF-Inp translocation is due to its 5′ phosphatase activity rather than by a non-enzymatic effect of the inducible translocation system.

We then determined whether this block in clathrin-mediated transferrin receptor endocytosis reflects a general suppression of membrane internalization. We investigated the effect of rapid PtdIns(4,5)P_2 depletion on fluid-phase endocytosis, a clathrin-independent process (Nichols and Lippincott-Schwartz, 2001). iRap-induced translocation of CF-Inp had no significant effect on the uptake of fluorescein-Dextran (M_r 10,000), whereas it blocked the uptake of transferrin in the same cell (Fig. 1E,F). This indicates that the requirement of PM PtdIns(4,5)P_2 is selective for clathrin-mediated endocytosis over fluid-phase endocytosis.

PtdIns(4,5)P_2 depletion increases transferrin receptor levels at the PM

Recent studies suggest that PtdIns(4,5)P_2 is involved not only in endocytosis but also in the recycling of endocytosed cargoes back to the PM (Cremona and De Camilli, 2001). For example, deletion of PIPKIγ, the major PtdIns(4,5)P_2-synthesizing enzyme in the brain, leads to defects in synaptic vesicle recycling (Di Paolo et al., 2004). In non-neuronal cells, the involvement of PtdIns(4,5)P_2 in the endosomal recycling pathway has been implicated from

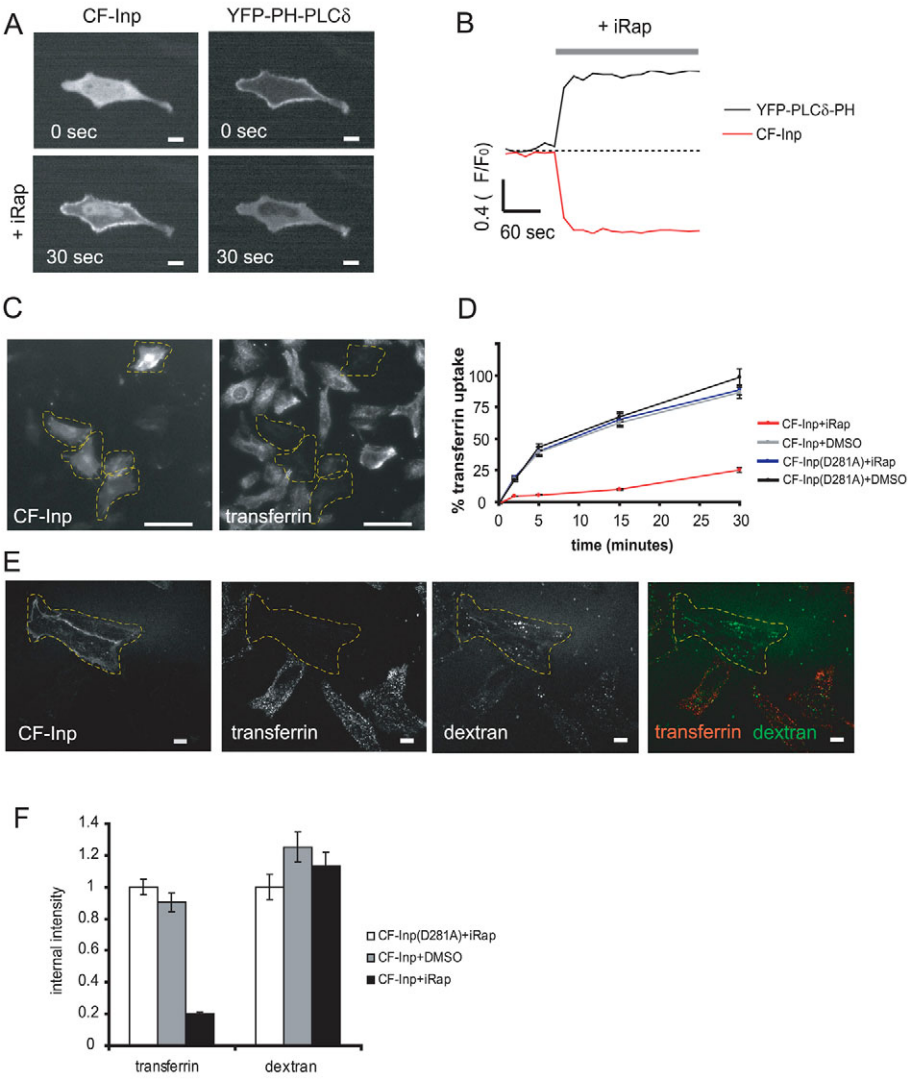

Fig. 1. PM PtdIns(4,5)P_2 hydrolysis disrupts endocytosis of the transferrin receptor, but not fluid-phase endocytosis. (A,B) iRap induces rapid translocation of CFP-FKBP-Inp (CF-Inp) from the cytosol to the PM and dissociation of PtdIns(4,5)P_2 biosensor YFP-PLCδ-PH from the PM. Sample image (A), and corresponding time course of CF-Inp and YFP-PLCδ-PH translocation (B). Scale bars: 10 µm. (C,D) Rapid PtdIns(4,5)P_2 hydrolysis inhibits transferrin uptake. HeLa cells expressing Lyn-FRB and either CF-Inp or CF-Inp(D281A) were treated with iRap or DMSO for 1 minute before addition of Alexa-Fluor-594-conjugated transferrin. (C) Sample image of CF-Inp-expressing cells treated with iRap and fixed after 15 minutes of Alexa-Fluor-594-conjugated-transferrin uptake. Dashed area indicates the location of Lyn-FRB- and CF-Inp-expressing cells. Scale bars: 50 µm. (D) Time-course of Alexa-Fluor-594-conjugated-transferrin uptake (significance of difference $P<9\times10^{-46}$ at the 15-minute time point). Error bars represent s.e.m. (E,F) Rapid PtdIns(4,5)P_2 hydrolysis does not affect dextran uptake. Following treatment with either DMSO or iRap, cells expressing Lyn-FRB and CF-Inp were assayed for internalization of Alexa-Fluor-594-conjugated transferrin and fluorescein-dextran simultaneously. (E) Representative image of CF-Inp-expressing cells treated with iRap and fixed after Alexa-Fluor-594-conjugated-transferrin and fluorescein-dextran uptake. Dashed area indicates the location of Lyn-FRB- and CF-Inp-expressing cells. Scale bars: 10 µm. (F) Quantification of transferrin and dextran uptake. For each tracer, the intracellular fluorescence intensity was normalized to that measured in cells expressing Lyn-FRB and CF-Inp(D281A) that were treated with iRap. Error bars represent s.e.m.

experiments in which the 5-phosphatase domain of synaptojanin was overexpressed, which in turn reduced the recycling rate of transferrin receptors (Kim et al., 2006). Although these studies suggest that prolonged changes in PtdIns(4,5)P_2 levels cause defects in endosomal recycling, it can not be excluded that the observed effects on recycling are caused by indirect regulatory mechanisms or defects occurring elsewhere, not at the PM.

We tested the role of PM PtdIns(4,5)P_2 in the recycling process by reducing PM PtdIns(4,5)P_2 levels after having loaded the endocytic compartments with fluorescently labeled transferrin. We incubated HeLa cells for 20 minutes with Alexa-Fluor-594-conjugated transferrin before inducing PM PtdIns(4,5)P_2 hydrolysis. Recycling of internalized transferrin receptors was monitored by the loss of internal Alexa-Fluor-594-conjugated transferrin fluorescence as the ligand-receptor complex returned to the cell surface. PM PtdIns(4,5)P_2 hydrolysis following transferrin uptake caused a partial block of the reinsertion of Alexa-Fluor-594-conjugated transferrin fluorescence (Fig. 2A,B). A fraction of Alexa-Fluor-594-conjugated transferrin fluorescence appeared to accumulate both in endosomes and near the PM, suggesting that receptor-containing vesicles are less effective in fusing with the PM (Fig. 2A). In control experiments, PM translocation of the CF-Inp(D281A) phosphatase-dead mutant had no effect on recycling.

To assess the relative effect of PtdIns(4,5)P_2 hydrolysis on endocytosis versus that on recycling, we monitored the amount of transferrin receptors expressed at the cell surface. Using an antibody against the extracellular domain of the transferrin receptor, we found a 50% increase in the amount of receptor expressed at the PM after

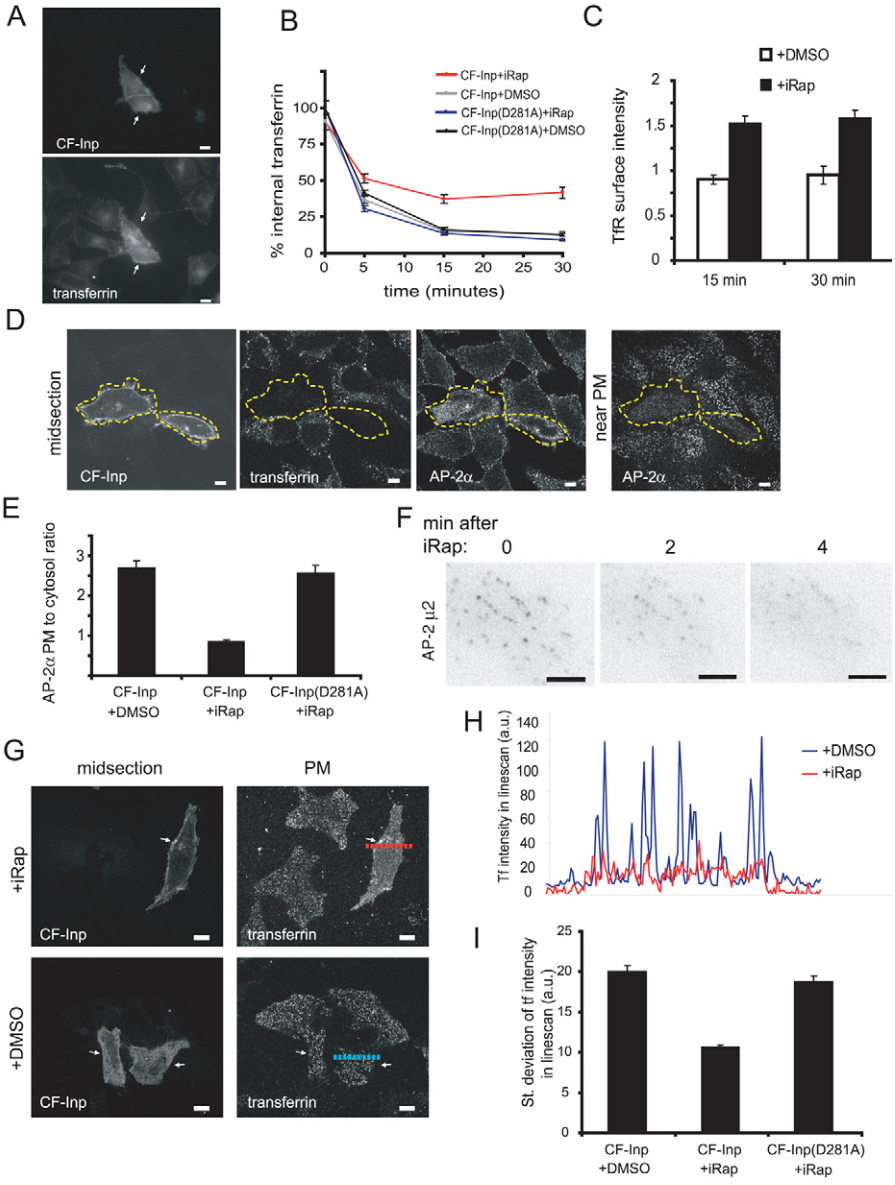

Fig. 2. PM PtdIns(4,5)P_2 hydrolysis partially inhibits transferrin receptor recycling to the surface while fully suppressing AP-2α PM localization and targeting of transferrin receptor (TfR) to endocytic sites. (A,B) Rapid PtdIns(4,5)P_2 hydrolysis causes partial inhibition of the reinsertion of internalized transferrin receptors back to the cell surface. Cells expressing Lyn-FRB and either CF-Inp or CF-Inp(D281A) were treated with Alexa-Fluor-594-conjugated transferrin for 20 minutes, then kept in Alexa-Fluor-594-conjugated-transferrin-free media for an additional 5, 15 or 30 minutes with iRap or DMSO. (A) Internal Alexa-Fluor-594-conjugated transferrin remaining in CF-Inp-translocated cells after 15 minutes of recycling. Arrows point to Lyn-FRB- and CF-Inp-expressing cells. Scale bars: 10 μm. (B) Time course of internal transferrin loss. Intracellular fluorescence intensity was normalized to that measured in cells expressing Lyn-FRB and CF-Inp(D281A) that were fixed immediately after Alexa-Fluor-594-conjugated-transferrin uptake without recycling (significance of difference $P<7\times10^{-11}$ at the 15-minute time point). Error bars represent s.e.m. (C) Rapid PtdIns(4,5)P_2 hydrolysis increases the amount of transferrin receptors expressed at the PM, suggesting that PtdIns(4,5)P_2 regulates endocytosis significantly more than it does recycling. Cells expressing Lyn-FRB and CF-Inp were treated with iRap or DMSO for 15 or 30 minutes, then stained with transferrin receptor antibody to label surface transferrin receptors. Receptor expression is normalized to the fluorescence intensity measured in cells without iRap or DMSO treatment. Error bars represent s.e.m. (D) Antibody against AP-2α shows that PtdIns(4,5)P_2 depletion causes a dissociation of AP-2α puncta from the PM. Cells expressing Lyn-FRB and CF-Inp were treated with Alexa-Fluor-594-conjugated transferrin for 5 minutes following a 1-minute treatment with iRap. Dashed area indicates the location of Lyn-FRB- and CF-Inp-expressing cells. Scale bars: 10 μm. (E) Quantitative analysis of the PM dissociation of AP-2α using ratio imaging of the fluorescence intensity near the PM versus that of the midsection. Error bars represent s.e.m. (F) TIRF imaging of AP-2-μ2–YFP fluorescence at the PM better resolves the rapid loss of AP-2-μ2-YFP from the PM upon iRap-induced translocation of CF-Inp. Scale bars: 5 μm. (G-I) The AP-2-adaptor-mediated clustering of transferrin receptors is also lost upon PtdIns(4,5)P_2 hydrolysis. Cells expressing Lyn-FRB and either CF-Inp or CF-Inp(D281A) were treated with either DMSO or iRap for 5 minutes, then incubated with Alexa-Fluor-594-conjugated transferrin at 4°C to label transferrin receptors at the surface. Representative images are shown in G. Arrows point to Lyn-FRB- and CF-Inp-expressing cells. Scale bar: 10 μm. (H) Linescan of transferrin intensity from broken lines drawn in G reveals the loss of sharp peaks of transferrin intensity upon PtdIns(4,5)P_2 hydrolysis. (I) Mean of the standard deviations of transferrin intensity calculated from each linescan collected. Error bars represent s.e.m.

15 minutes of PtdIns(4,5)P_2 hydrolysis (Fig. 2C). There was no further increase in antibody fluorescence intensity after 30 minutes of hydrolysis, indicating that the recycling was blocked after 15 minutes. Assuming that synthesis of new receptors is negligible within the time-scale of minutes, the concentration of surface receptors is a direct function of the ratio between the endocytosis and recycling rates. Thus, the net increase in the level of transferrin receptor at the PM upon PtdIns(4,5)P_2 hydrolysis suggests that endocytosis and recycling have different sensitivities to PtdIns(4,5)P_2 reduction. PtdIns(4,5)P_2 can therefore directly regulate the surface expression of transferrin receptor by first suppressing endocytosis before interfering with the recycling process.

PtdIns(4,5)P_2 depletion dissociates AP-2 from the PM

Because PtdIns(4,5)P_2 has an indispensable role for transferrin receptor endocytosis, we focused our investigation on the molecular mechanism by which PtdIns(4,5)P_2 regulates this process. One proposed role of PM PtdIns(4,5)P_2 in clathrin-mediated endocytosis is in the recruitment of endocytic components to sites of endocytosis. Previous studies suggest that proteins important for the assembly of clathrin-coated vesicles bind to PtdIns(4,5)P_2 preferentially over other phosphoinositides, and local increases in PtdIns(4,5)P_2 serve as a key step in promoting receptor assembly in clathrin-coated pits (Krauss et al., 2003; Doughman et al., 2003). An important mediator of this assembly process is AP-2, which binds to various endocytosed receptors, clathrin and clathrin-coated-vesicle-associated proteins (Owen et al., 2004). Previous studies indicate that PtdIns(4,5)P_2 plays a role in the recruitment of AP-2 to endocytic sites at the PM. Mutant AP-2 with a deletion in the putative lipid-binding domain fail to localize to clathrin-coated pits (Gaidarov and Keen, 1999). In vitro studies suggest that PtdIns(4,5)P_2 is required for AP-2 to interact with the endocytic cargo (Honing et al., 2005). Furthermore, knockdown of phosphatidylinositol phosphate 5-kinase Iβ, an enzyme that produces PtdIns(4,5)P_2, leads to a reduction of membrane-localized AP-2 (Padron et al., 2003). Rapid depletion of PM PtdIns(4,5)P_2 with 1-butanol or another inducible 5′-phosphatase translocation strategy was also shown to lead to a dissociation of AP-2 from the PM (Boucrot et al., 2006; Zoncu et al., 2007).

We used the PtdIns(4,5)P_2-specific Inp54p PM translocation system to confirm such a role of PtdIns(4,5)P_2 in AP-2 PM targeting using immunofluorescence and live total internal reflectance fluorescence (TIRF) microscopy. The distribution of AP-2α immunofluorescence observed in PtdIns(4,5)P_2-hydrolyzed cells was diffuse and cytosolic, in contrast to the punctate distribution near the PM observed in non-hydrolyzed control cells (Fig. 2D). The ratio of the average fluorescence intensity of AP-2α near the PM versus that in the midsection of the cell provides a quantitative measure for the loss of PM association of AP-2α upon PtdIns(4,5)P_2 hydrolysis (Fig. 2E). We further confirmed this effect using live TIRF imaging of YFP-tagged AP-2 μ2, a different component of the AP-2 adaptor complex. PtdIns(4,5)P_2 hydrolysis caused a rapid dissociation of AP-2-μ2–YFP from the PM within seconds, and a near complete loss by ~3-4 minutes (Fig. 2F). This finding that PtdIns(4,5)P_2 reduction leads to dissociation of AP-2 from the PM in less than 15 seconds supports the hypothesis that PtdIns(4,5)P_2 is directly required for targeting of AP-2 to the PM.

PtdIns(4,5)P_2 depletion prevents transferrin receptor clustering

Because AP-2 serves as an adaptor that directs receptors to clathrin-coated pits, we tested the effect of PtdIns(4,5)P_2 hydrolysis on transferrin receptor clustering. To visualize the localization of transferrin receptors at the PM, we incubated cells with Alexa-Fluor-594-conjugated transferrin at 4°C to label surface transferrin receptors. At this temperature, internalization of the ligand-receptor complex is inhibited. In PtdIns(4,5)P_2-hydrolyzed cells, we observed a uniform distribution of transferrin receptor compared with the punctate pattern observed in control cells (Fig. 2G). This effect was analyzed quantitatively using linescan analysis. Transferrin fluorescence intensity linescans showed sharp peaks in DMSO-treated control cells, reflecting the clustered distribution of

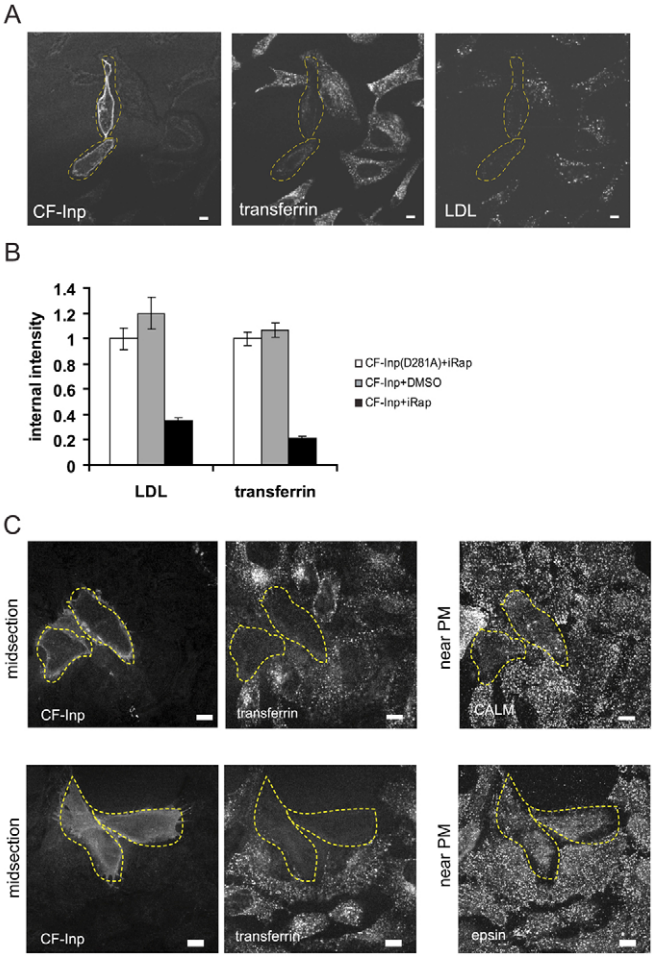

Fig. 3. PM PtdIns(4,5)P_2 hydrolysis significantly suppresses LDL receptor endocytosis and weakly suppresses PM localization of epsin and CALM adaptors. (A,B) Following treatment with either DMSO or iRap, cells expressing Lyn-FRB and CF-Inp were simultaneously assayed for internalization of DiI-labeled LDL and Alexa-Fluor-488-conjugated transferrin. (A) Representative image of CF-Inp-expressing cells treated with iRap and fixed after transferrin and LDL uptake, showing suppression of the internalization of both receptors in the same cells. Dashed area indicates the location of Lyn-FRB- and CF-Inp-expressing cells. Scale bars: 10 μm. (B) Quantification of transferrin and LDL uptake. For each tracer, the intracellular fluorescence intensity was normalized to that measured in cells expressing Lyn-FRB and CF-Inp(D281A) treated with iRap. Error bars represent s.e.m. (C) Antibody against CALM (top row) or epsin (bottom row) reveals PM-associated punctate localization in untransfected control cells but a more cytosolic distribution in PtdIns(4,5)P_2-depleted cells. Cells expressing Lyn-FRB and CF-Inp were treated with Alexa-Fluor-594-conjugated transferrin for 5 minutes following a 1-minute treatment with iRap. Dashed lines indicate the location of Lyn-FRB- and CF-Inp-expressing cells. Scale bars: 10 μm.

transferrin receptors in clathrin-coated pits (Fig. 2H). Linescans across PtdIns(4,5)P_2-hydrolyzed cells lacked these peaks, reflecting a uniform distribution of transferrin receptors (Fig. 2H). We also calculated the standard deviation of transferrin receptor intensity values within each linescan using normalized fluorescence. Standard-deviation values of transferrin intensity in linescans across PtdIns(4,5)P_2-hydrolyzed cells were markedly smaller than those measured in control cells (Fig. 2I). Thus, PtdIns(4,5)P_2 is required not only for targeting AP-2 to the PM but also for the clustering of transferrin receptors into clathrin-coated pits. These findings support a model in which PtdIns(4,5)P_2 targets AP-2 to the PM and that PM-localized AP-2 is required to direct transferrin receptors to clathrin-coated pits.

PtdIns(4,5)P_2 regulates LDL receptor endocytosis

We tested whether PtdIns(4,5)P_2 has also a role in regulating the endocytosis of low density lipoprotein (LDL) receptors and endocytosis of the endocytic coat components CALM and epsin. Even though LDL receptors are mostly endocytosed by an AP-2-independent endocytic route, we found that its endocytosis was also suppressed by PtdIns(4,5)P_2 hydrolysis (Fig. 3A). A comparison of the relative suppression of endocytosis of transferrin receptors versus LDL receptors is shown in Fig. 3B. Furthermore, antibodies against the alternative adaptor proteins epsin and CALM revealed a partial loss from the PM in PtdIns(4,5)P_2-depleted cells (Fig. 3C). This argues that PtdIns(4,5)P_2 regulates the endocytosis of a range of receptors, possibly by regulating, with different efficiency, different endocytic adaptors.

Assembly of PM clathrin is only weakly affected by PtdIns(4,5)P_2 depletion

In addition to its role in targeting receptors to coated pits, AP-2 has also been proposed to have a role in the assembly of clathrin coats at the PM (Gallusser and Kirchhausen, 1993; Shih et al., 1995; Brodsky et al., 2001). We tested the effect of reducing PtdIns(4,5)P_2 concentration on clathrin-coat assembly and disassembly at the PM using live TIRF imaging of YFP-tagged clathrin light chain (CLC). We added Alexa-Fluor-594-conjugated transferrin at the same time as iRap was added, and analyzed those cells in which transferrin uptake was significantly reduced. Surprisingly, iRap-induced translocation of CFInp led to only an approximately 20% reduction in the average intensity of clathrin puncta detected at the PM, suggesting that much of the clathrin remains clustered at the PM when PtdIns(4,5)P_2-levels were reduced after translocation of Inp54 (Fig. 4A,B, supplementary material Fig. S1).

Under these conditions, reduction in the number of detectable AP-2-2 μ2 puncta was more than fourfold stronger compared to that of clathrin puncta (Fig. 4C). Dynamic formation of new clathrin puncta was also still observed after iRap addition (supplementary material Movie 1). Furthermore, we did not observe a statistically significant change in the average lifetime of clathrin puncta upon hydrolysis of PtdIns(4,5)P_2 (52±3 seconds before iRap treatment, 47±3 seconds with iRap treatment) (Fig. 4D).

An earlier study reported that PtdIns(4,5)P_2 depletion with ionomycin, a strong activator of phospholipase C, or PM translocation of human 5′ phosphatase nearly completely blocks clathrin assembly (Zoncu et al., 2007). We confirmed their findings that addition of ionomycin suppresses dynamic clathrin assembly (supplementary material Movie 1). A plausible explanation for the discrepancy between their results and ours is a higher degree of PtdIns(4,5)P_2 depletion in their study resulting from the use of ionomycin or of the different 5′ phosphatase enzyme system they used. It is in this context useful to mention that experimentally observed receptor-mediated reductions in PtdIns(4,5)P_2 concentrations are believed to be graded and typically incomplete (i.e. Stauffer et al., 1998), and an important

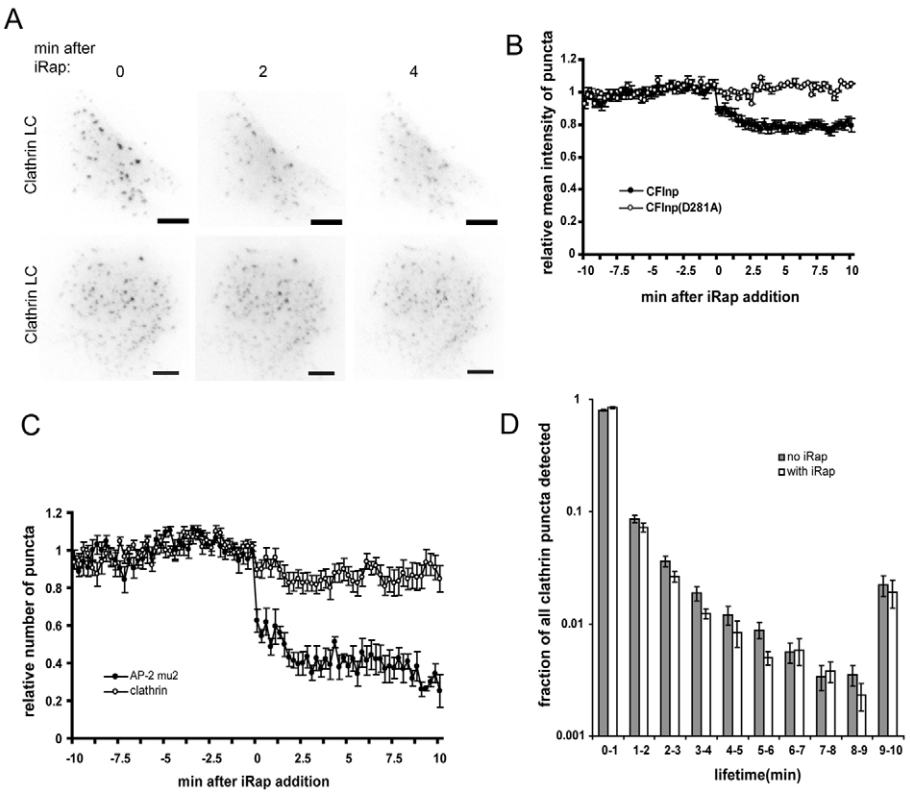

Fig. 4. PtdIns(4,5)P_2 hydrolysis has a much smaller effect on clathrin assembly at the PM compared to its effect on dissociating AP-2 adaptors. (A) TIRF imaging of YFP-CLC fluorescence shows only a partial loss of CLC at the PM upon iRap-induced translocation of CF-Inp. Scale bars: 5 μm. (B) PtdIns(4,5)P_2 hydrolysis resulted in only an ~20% reduction in mean clathrin-puncta intensity at the PM. Mean intensity value for each time point was normalized to the maximum mean intensity value measured in each cell. Error bars represent s.e.m. (C) Comparison of the number of puncta at each time point observed for AP-2-μ2–YFP or YFP-CLC after iRap-induced translocation of CF-Inp. Number of puncta was normalized to the maximum number detected in each cell. PtdIns(4,5)P_2 hydrolysis caused a more than fourfold greater effect on the number of AP-2-μ2–YFP-positive puncta compared with that on YFP-CLC-positive puncta. Errors represent s.e.m. (D) Normalized histogram of the lifetimes of YFP-CLC-positive puncta before and after iRap-induced translocation of CF-Inp. There was no significant reduction in the lifetime of CLC-positive puncta in iRap-treated cells. Errors represent s.e.m.

issue for understanding PtdIns(4,5)P_2 signaling is whether different PtdIns(4,5)P_2-regulated processes have different sensitivities to PtdIns(4,5)P_2. Our study argues that physiological reductions in PtdIns(4,5)P_2 primarily act on adaptor proteins such as AP-2 and thereby reduce the targeting of cargo to endocytic sites, whereas supramaximal reductions in PtdIns(4,5)P_2 are needed to interfere with clathrin assembly or with receptor recycling back to the surface.

Conclusion

We conclude that PtdIns(4,5)P_2 is required for transferrin receptor endocytosis, but not for fluid-phase endocytosis. Furthermore, although PtdIns(4,5)P_2 plays a vital role in endocytosis, reductions in PtdIns(4,5)P_2 have less of an effect on receptor recycling back to the surface. This differential role of PtdIns(4,5)P_2 in endocytosis versus recycling leads to an increase in the amount of transferrin receptor in the PM following PtdIns(4,5)P_2 reduction. Furthermore, our results suggest that a primary role of physiological decreases in PtdIns(4,5)P_2 for endocytosis is a strong PM dissociation of adaptor complex AP-2, and a weaker PM dissociation of the adaptor proteins epsin and CALM. This is consistent with a model in which receptor-mediated increases or decreases in the concentration of PtdIns(4,5)P_2 control the PM localization of endocytic adaptors and thereby enhance or reduce the adaptor-mediated delivery of receptor cargo to endocytic sites. Based on our findings, the dynamic assembly of clathrin at the PM is much less affected by decreases in PtdIns(4,5)P_2 concentration compared with the effects on AP-2, suggesting that physiological changes in PtdIns(4,5)P_2 regulate adaptor-mediated targeting of cargo to endocytic sites rather than clathrin assembly.

Materials and Methods

Cell culture, transfection and constructs

HeLa cells were purchased from ATCC, and cultured in DMEM containing 10% FBS and 1% Penicillin-Streptomycin-Glutamine at 37°C at 10% CO_2. Cells were plated on Costar 96-well flat-bottom plates for epifluorescence microscopy. For confocal microscopy, cells were plated on 8-well labtek coverslips (Nunc). 24 hours after plating, cells were transfected with FuGENE6 (Roche). All experiments were performed 18-20 hours after transfection. YFP-PLCδ-PH (Stauffer et al., 1998), Lyn_{11}-FRB, CFP-FKBP-Inp54p and CFP-FKBP-Inp54p(D281A) (Suh et al., 2006) constructs are previously described. Construct requests should be made to T.I. (jctinoue@stanford.edu). AP-2-μ2–YFP was a kind gift from Alexander Sorkin (University of Colorado, CO) and YFP-CLC was a kind gift from Juan Bonifacino (NICHD, National Institute of Health, MD).

Live microscopy

CF-Inp and YFP-PLCδ-PH translocation was monitored by live imaging with a 40× objective (Zeiss) on a spinning-disk confocal microscope (Nipkow Wallac system). Images were analyzed with MetaMorph 6.1 software (Universal Imaging).

Objective-based TIRF imaging of YFP-CLC and AP-2-μ2–YFP was performed with a NA 1.45 100× objective (Zeiss) on an inverted microscope (Zeiss) at 37°C. For each cell, YFP TIRF images were obtained every 15 seconds for 10 minutes, followed by addition of 5 μg/ml Alexa-Fluor-594-conjugated transferrin and 5 μM iRap. After addition, YFP TIRF images were obtained every 15 seconds for 10 minutes or until complete dissociation was observed. Alexa-Fluor-594-conjugated-transferrin uptake was imaged using epifluorescence at the end of each experiment.

Internalization and recycling assays

All internalization and recycling assays were performed at 37°C. Prior to the transferrin-internalization assay, transferrin present in serum was removed by two washes with DMEM (with 25 mM HEPES, GIBCO). Cells were then incubated with 5 μM iRap in DMEM-HEPES or 0.1% DMSO in DMEM-HEPES. 1 minute later, Alexa-Fluor-594-conjugated transferrin (Invitrogen) in DMEM-HEPES was added to the iRap or DMSO solution to a final concentration of 5 μg/ml Alexa-Fluor-594-conjugated transferrin. After 2, 5, 15 or 30 minutes, extracellular Alexa-Fluor-594-conjugated transferrin was removed by ice-cold acid solution containing 0.2 M acetic acid and 0.5 M NaCl, followed by neutralization with DPBS (GIBCO). Cells were then fixed with 4% formaldehyde (Ted Pella) in PBS for 10 minutes at room temperature.

For the transferrin receptor recycling assay, cells were first washed twice with DMEM-HEPES, then incubated with 5 μg/ml Alexa-Fluor-594-conjugated transferrin for 20 minutes. Extracellular Alexa-Fluor-594-conjugated transferrin was then removed with acid solution containing 0.2 M acetic acid and 0.5 M NaCl, followed by DPBS neutralization. Cells were then incubated in 5 μM iRap or 0.1% DMSO in DMEM-HEPES containing 50 μg/ml holotransferrin (Sigma). Cells were fixed with 4% formaldehyde in PBS after 5, 15 or 30 minutes. For both the internalization and recycling assays, Alexa-Fluor-594-conjugated transferrin and CF-Inp/CF-Inp(D281A) fluorescence was imaged with a 20× objective (Nikon) on an automated epi-fluorescent microscope ImageXpress 5000A (Molecular Devices). Fluorescence intensities of single cells were measured with the ImageXpress analysis software.

For dextran and transferrin internalization, cells were first washed twice with DMEM and incubated with 5 μM iRap in DMEM-HEPES or 0.1% DMSO in DMEM-HEPES. 1 minute later, fluorescein-dextran (Invitrogen) and Alexa-Fluor-594-conjugated transferrin in DMEM-HEPES were added to the iRap or DMSO solution to a final concentration of 10 mg/ml fluorescein-dextran and 5 μg/ml Alexa-Fluor-594-conjugated transferrin. After 20 minutes of uptake, extracellular Alexa-Fluor-594-conjugated transferrin was removed by ice-cold acid solution containing 0.2 M acetic acid and 0.5 M NaCl, followed by neutralization with DPBS (GIBCO). Cells were then fixed with 4% formaldehyde (Ted Pella) in PBS for 10 minutes at room temperature. DiI-LDL and transferrin internalization were performed similarly, with 5 μg/ml DiI-LDL and 5 μg/ml Alexa-Fluor-488-conjugated transferrin. Alexa-Fluor-594-conjugated transferrin, fluorescein-dextran, DiI-LDL and CF-Inp/CF-Inp(D281A) fluorescence were imaged with a 63× objective (Zeiss) on the Bio-Rad Radiance 2100 Laser-scanning confocal system. Images were taken from the midsection of the cell. Parameters on camera and microscope were set so that no area was saturated, and the same setting was used to image all cells. Images were analyzed with MetaMorph 6.1 software (Universal Imaging). The background fluorescence of each image was subtracted before analysis.

Immunofluorescence

To label surface transferrin receptors, anti-transferrin-receptor antibody staining was performed using live cells at 4°C to prevent receptor internalization. Cells were pre-incubated at 4°C in DMEM-HEPES for 10 minutes. Then, cells were immunostained with mouse anti-human CD71 in DMEM-HEPES with 1% BSA (1:1000; BD Pharmingen) for 45 minutes. Cells were then fixed for 10 minutes with 4% formaldehyde in PBS at room temperature and stained with goat anti-mouse IgG conjugated to Alexa-Fluor-568 (1:1000; Invitrogen). Fluorescence was imaged with a 20× objective on ImageXpress 5000A (Molecular Devices) and fluorescence intensities of single cells were measured with the ImageXpress analysis software.

To label intracellular antigens, cells were fixed with 4% formaldehyde and permeabilized with 0.1% Triton-X 100, followed by staining with mouse anti-AP-2α (1:1000; Calbiochem), goat anti-epsin-1 (1:200; Santa Cruz Biotechnology), or goat anti-CALM (1:200; Santa Cruz Biotechnology) for 45 minutes in PBS with 1% BSA. Secondary antibody staining was performed with Alexa-Fluor-568-conjugated or Alexa-Fluor-488-conjugated goat anti-mouse IgG in PBS with 1% BSA (1:1000). Confocal images were taken with a 63× objective (Zeiss) on the Bio-Rad Radiance 2100 Laser-scanning confocal system. Images were analyzed with MetaMorph 6.1 software (Universal Imaging). The background fluorescence of each image was subtracted before analysis. The PM:cytosol ratio of AP-2α was measured by dividing the average fluorescence intensity measured from the bottom section of the cell (near the PM) with that measured from the midsection of the cell.

Binding of fluorescently labeled transferrin on live cells

Labeling of surface transferrin receptors with Alexa-Fluor-594-conjugated transferrin was performed at 4°C to prevent internalization. After a 5-minute incubation with either 5 μM iRap or 0.1% DMSO in DMEM-HEPES at 37°C, cells were washed with cold DMEM-HEPES and placed at 4°C for 10 minutes. Cells were then incubated with 5 μg/ml Alexa-Fluor-594-conjugated transferrin in DMEM-HEPES for 30 minutes at 4°C, followed by fixation with 4% formaldehyde for 10 minutes at 4°C. The PM section at the bottom of the cell was imaged with a 63× objective (Zeiss) on the Bio-Rad Radiance 2100 Laser-scanning confocal system.

Linescan analysis

Linescan analysis was performed with MetaMorph 6.1 software (Universal Imaging). The background fluorescence of each image was subtracted before analysis. The intensity of transferrin fluorescence in each cell was normalized so that the average intensity was the same for all cells. Three random linescans were taken across the width of each cell. The width of the line was approximately 1 μm. The standard deviation of the fluorescence intensity within each linescan was calculated.

Puncta analysis

MATLAB R2006b was used for puncta detection, intensity and lifetime analysis. For puncta detection, a gaussian filter was first applied to raw images, then local maxima corresponding to CCPs were detected. For puncta lifetime analysis, we used a tracking algorithm developed by John C. Crocker (University of Pennsylvania, PA).

Statistics

For Figs 1, 2 and Fig. 3B, we analyzed between 30 and 200 individual cells for each time point and condition. For linescan analysis, we took three linescans from each cell and used between 13 and 40 cells for each condition. For live TIRF imaging, we analyzed eight cells for AP-2-μ2–YFP and CFInp54 translocation, nine cells for YFP-CLC with CFInp54 translocation and three cells for YFP-CLC with CFInp(D281A) translocation.

We thank M. Fivaz for helpful discussions; and O. Brandman, P. Vitorino and M. Hammer for data analysis. N.A. is a recipient of the Stanford Bio-X Paul Berg graduate fellowship. T.I. is a recipient of a fellowship from the Quantitative Chemical Biology Program.

References

Brodsky, F. M., Chen, C. Y., Knuehl, C., Towler, M. C. and Wakeham, D. E. (2001). Biological basket weaving: formation and function of clathrin-coated vesicles. *Annu. Rev. Cell Dev. Biol.* **17**, 517-568.

Boucrot, E., Saffarian, S., Massol, R., Kirchhausen, T. and Ehrlich, M. (2006). Role of lipids and actin in the formation of clathrin-coated pits. *Exp. Cell Res.* **312**, 4036-4048.

Cremona, O. and De Camilli, P. (2001). Phosphoinositides in membrane traffic at the synapse. *J. Cell Sci.* **114**, 1041-1451.

Di Paolo, G. and De Camilli, P. (2006). Phosphoinositides in cell regulation and membrane dynamics. *Nature* **443**, 651-657.

Di Paolo, G., Moskowitz, H. S., Gipson, K., Wenk, M. R., Voronov, S., Obayashi, M., Flavell, R., Fitzsimonds, R. M., Ryan, T. A. and De Camilli, P. (2004). Impaired PtdIns(4,5)P_2 synthesis in nerve terminals produces defects in synaptic vesicle trafficking. *Nature* **431**, 415-422.

Doughman, R. L., Firestone, A. J. and Anderson, R. A. (2003). Phosphatidylinositol phosphate kinases put PI4,5P(2) in its place. *J. Membr. Biol.* **194**, 77-89.

Gaidarov, I. and Keen, J. H. (1999). Phosphoinositide-AP-2 interactions required for targeting to plasma membrane clathrin-coated pits. *J. Cell Biol.* **146**, 755-764.

Gallusser, A. and Kirchhausen, T. (1993). The beta 1 and beta 2 subunits of the AP complexes are the clathrin coat assembly components. *EMBO J.* **12**, 5237-5244.

Haucke, V. (2005). Phosphoinositide regulation of clathrin-mediated endocytosis. *Biochem. Soc. Trans.* **33**, 1285-1289.

Heo, W. D., Inoue, T., Park, W. S., Kim, M. L., Park, B. O., Wandless, T. J. and Meyer, T. (2006). PI(3,4,5)P_3 and PI(4,5)P_2 lipids target proteins with polybasic clusters to the plasma membrane. *Science* **314**, 1458-1461.

Hinrichsen, L., Harborth, J., Andrees, L., Weber, K. and Ungewickell, E. J. (2003). Effect of clathrin heavy chain- and alpha-adaptin-specific small inhibitory RNAs on endocytic accessory proteins and receptor trafficking in HeLa cells. *J. Biol. Chem.* **278**, 45160-45170.

Honing, S., Ricotta, D., Krauss, M., Spate, K., Spolaore, B., Motley, A., Robinson, M., Robinson, C., Haucke, V. and Owen, D. J. (2005). Phosphatidylinositol-(4,5)-bisphosphate regulates sorting signal recognition by the clathrin-associated adaptor complex AP2. *Mol. Cell* **18**, 519-531.

Inoue, T., Heo, W. D., Grimley, J. S., Wandless, T. J. and Meyer, T. (2005). An inducible translocation strategy to rapidly activate and inhibit small GTPase signaling pathways. *Nat. Methods* **2**, 415-418.

Kim, S., Kim, H., Chang, B., Ahn, N., Hwang, S., Di Paolo, G. and Chang, S. (2006). Regulation of transferrin recycling kinetics by PtdIns[4,5]P_2 availability. *FASEB J.* **20**, 2399-2401.

Krauss, M., Kinuta, M., Wenk, M. R., De Camilli, P., Takei, K. and Haucke, V. (2003). ARF6 stimulates clathrin/AP-2 recruitment to synaptic membranes by activating phosphatidylinositol phosphate kinase type Igamma. *J. Cell Biol.* **162**, 113-124.

Motley, A., Bright, N. A., Seaman, M. N. and Robinson, M. S. (2003). Clathrin-mediated endocytosis in AP-2-depleted cells. *J. Cell Biol.* **162**, 909-918.

Nichols, B. J. and Lippincott-Schwartz, J. (2001). Endocytosis without clathrin coats. *Trends Cell Biol.* **11**, 406-412.

Owen, D. J., Collins, B. M. and Evans, P. R. (2004). Adaptors for clathrin coats: structure and function. *Annu. Rev. Cell Dev. Biol.* **20**, 153-191.

Padron, D., Wang, Y. J., Yamamoto, M., Yin, H. and Roth, M. G. (2003). Phosphatidylinositol phosphate 5-kinase Ibeta recruits AP-2 to the plasma membrane and regulates rates of constitutive endocytosis. *J. Cell Biol.* **162**, 693-701.

Roth, M. G. (2004). Phosphoinositides in constitutive membrane traffic. *Physiol. Rev.* **84**, 699-730.

Shih, W., Gallusser, A. and Kirchhausen, T. (1995). A clathrin-binding site in the hinge of the beta 2 chain of mammalian AP-2 complexes. *J. Biol. Chem.* **270**, 31083-31090.

Stauffer, T. P., Ahn, S. and Meyer, T. (1998). Receptor-induced transient reduction in plasma membrane PtdIns(4,5)P_2 concentration monitored in living cells. *Curr. Biol.* **8**, 343-346.

Suh, B. C. and Hille, B. (2005). Regulation of ion channels by phosphatidylinositol 4,5-bisphosphate. *Curr. Opin. Neurobiol.* **15**, 370-378.

Suh, B. C., Inoue, T., Meyer, T. and Hille, B. (2006). Rapid chemically induced changes of PtdIns(4,5)P_2 gate KCNQ ion channels. *Science* **314**, 1454-1457.

Tsujishita, Y., Guo, S., Stolz, L. E., York, J. D. and Hurley, J. H. (2001). Specificity determinants in phosphoinositide dephosphorylation: crystal structure of an archetypal inositol polyphosphate 5-phosphatase. *Cell* **105**, 379-389.

Varnai, P., Thyagarajan, B., Rohacs, T. and Balla, T. (2006). Rapidly inducible changes in phosphatidylinositol 4,5-bisphosphate levels influence multiple regulatory functions of the lipid in intact living cells. *J. Cell Biol.* **175**, 377-382.

Zoncu, R., Perera, R. M., Sebastian, R., Nakatsu, F., Chen, H., Balla, T., Ayala, G., Toomre, D. and De Camilli, P. V. (2007). Loss of endocytic clathrin-coated pits upon acute depletion of phosphatidylinositol 4,5-bisphosphate. *Proc. Natl. Acad. Sci. USA* **104**, 3793-3798.